Configuration-constrained cranking Hartree-Fock pairing calculations for sidebands of nuclei

W. Y. Liang (梁午阳),[1] C. F. Jiao (焦长峰),[1] Q. Wu (吴强),[1] X. M. Fu (付熙明),[1,2] and F. R. Xu (许甫荣)[1,3,*]

[1]*State Key Laboratory of Nuclear Physics and Technology, School of Physics, Peking University, Beijing 100871, China*

[2]*National Institute for Radiological Protection, Chinese Center for Disease Control and Prevention, Beijing 100088, China*

[3]*State Key Laboratory of Theoretical Physics, Institute of Theoretical Physics, Chinese Academy of Science, Beijing 100190, China*

(Received 10 September 2015; revised manuscript received 8 November 2015; published 29 December 2015)

Background: Nuclear collective rotations have been successfully described by the cranking Hartree-Fock-Bogoliubov (HFB) model. However, for rotational sidebands which are built on intrinsic excited configurations, it may not be easy to find converged cranking HFB solutions. The nonconservation of the particle number in the BCS pairing is another shortcoming. To improve the pairing treatment, a particle-number-conserving (PNC) pairing method was suggested. But the existing PNC calculations were performed within a phenomenological one-body potential (e.g., Nilsson or Woods-Saxon) in which one has to deal the double-counting problem.

Purpose: The present work aims at an improved description of nuclear rotations, particularly for the rotations of excited configurations, i.e., sidebands.

Methods: We developed a configuration-constrained cranking Skyrme Hartree-Fock (SHF) calculation with the pairing correlation treated by the PNC method. The PNC pairing takes the philosophy of the shell model which diagonalizes the Hamiltonian in a truncated model space. The cranked deformed SHF basis provides a small but efficient model space for the PNC diagonalization.

Results: We have applied the present method to the calculations of collective rotations of hafnium isotopes for both ground-state bands and sidebands, reproducing well experimental observations. The first up-bendings observed in the yrast bands of the hafnium isotopes are reproduced, and the second up-bendings are predicted. Calculations for rotational bands built on broken-pair excited configurations agree well with experimental data. The band-mixing between two $K^\pi = 6^+$ bands observed in ^{176}Hf and the K purity of the ^{178}Hf rotational state built on the famous 31 yr $K^\pi = 16^+$ isomer are discussed.

Conclusions: The developed configuration-constrained cranking calculation has been proved to be a powerful tool to describe both the yrast bands and sidebands of deformed nuclei. The analyses of rotational moments of inertia help to understand the structures of nuclei, including rotational alignments, configurations, and competitions between collective and single-particle excitations.

DOI: 10.1103/PhysRevC.92.064325 PACS number(s): 21.10.Re, 21.60.Ev, 21.60.Jz, 27.70.+q

I. INTRODUCTION

Cranking calculations with phenomenological one-body potentials (e.g., Nilsson, Woods-Saxon) or effective two-body forces (e.g., Skyrme force or relativistic mean field) have been successful in the description of nuclear collective rotations. In cranking calculations, the self-consistence in pairing and deformation plays an important role in explaining experimental observations [1]. However, the self-consistent numerical calculation of the cranking HFB approach is difficult when it is applied to multiquasiparticle (multi-qp) rotations where pairing is reduced remarkably. It was pointed out that, in band-crossing regions, special attention is needed in the numerical iteration of the cranking calculations [2]. Most of existing cranking HFB calculations are for the yrast bands. Pairing calculations based on microscopic two-body forces are still lacking for sidebands.

In the HFB model, the particle number is not conserved. The spurious pairing collapse (also called spurious pairing phase transition) arising from the cranking HFB calculations [3–6] would be related to the violation of the particle number conservation. As well, the spurious phase transition occurs in band-crossing regions [7,8]. It was addressed that the phase transition cannot be described properly in mean-field methods for finite systems, due to the particle-number fluctuation [9,10]. To consider the effect from the particle number fluctuation, one can project the HFB wave function onto a good particle number before variation [11–13]. But it greatly complicates the algorithm and sometimes fails to describe the high-lying part of the rotational spectrum [14]. Although the approximate particle-number-projected Lipkin-Nogami (LN) pairing method improves the cranking HFB solution, the problem of the spurious phase transition is not fully solved for the rotations of exited configurations where the pairing is reduced significantly [15,16].

To overcome the particle-number fluctuation problem, a particle-number-conserving (PNC) pairing method was developed [17] and has been successfully applied to cranking calculations [18–20]. The PNC pairing method has the concept of the "standard" shell model which diagonalizes the Hamiltonian within a truncated model space. Different from the numerical iterations of the cranking HFB equations, the diagonalization easily gives a numerical solution, and its convergence can be checked against the model dimension chosen. Due to taking a cranked deformed basis, the cranking PNC calculation has a fast convergence against the model dimension. Usually a dimension of 800–1000 should be

*frxu@pku.edu.cn

enough for the spectroscopic calculations of heavy nuclei [16,21]. Furthermore, the PNC method defines configurations in a single-particle basis similar to shell model, and therefore exact blocking calculation can be easily done by blocking the specific single-particle orbits in wave functions. In the Bogoliubov pairing, one usually blocks quasiparticle orbits, because it gets very complicated to use a single-particle scheme for unpaired particles and a quasiparticle scheme for paired particles in one framework of the model. But in principle, one should block real-particle orbits (i.e., single particles) that specify the configuration of a state, which is important for the calculations of broken-pair states [16,18].

Previous cranking PNC calculations were performed with the Nilsson potential (e.g., in Refs. [18–20,22]). The calculation was performed with a fixed deformation [18–20], and the result is dependent on which deformation is taken. The choice of deformation parameters relies somewhat on data usually, which limits the predictive power of the model. Moreover, deformations can vary with increasing angular momentum or with changing configuration. The deformation variation and incurred effects can be remarkable in soft nuclei. Therefore, a self-consistent deformation which is determined by the model itself is desired. In our recent works [16,23], we have replaced the Bogoliubov pairing by the PNC pairing in the total-Routhian-surface (TRS) method with the Woods-Saxon potential adopted. The self-consistent deformation is determined by minimizing the calculated TRS at each given rotational frequency [16,23]. A significant improvement for rotational calculations is obtained [16,23]. The calculations give the evolution of the rotational behavior with increasing angular momentum and/or with changing configuration [16,23].

However, the Hamiltonian based on a one-body potential raises the double counting problem. Usually, we use the Strutinsky method to remove the double-counting problem approximately. But in the TRS method, the energy change due to rotation is simply written as $\langle\Psi^\omega|\hat{H}^\omega|\Psi^\omega\rangle - \langle\Psi^\omega|\hat{H}^\omega|\Psi^\omega\rangle^{\omega=0}$ [1,24]. Although the double counting effect should be largely canceled by calculating the energy difference between frequencies ω and zero, it is not removed exactly. The double counting problem does not appear in models based on the Hartree-Fock (HF) approximation with a two-body nuclear force (e.g., Skyrme or Gogny force), in which the energy of the many-body system is not simply written as a summation of single-particle energies. In the present work, we incorporate the PNC pairing into the Skyrme HF (SHF) model. We mainly focus on the rotational sidebands of deformed nuclei.

II. THE MODEL

Using the second quantization, we write the cranked many-body Hamiltonian of nucleus as

$$\hat{H}^\omega = \sum_{ij} t_{ij} a_i^\dagger a_j + \frac{1}{4}\sum_{ijkl} \overline{V}_{ijkl} a_i^\dagger a_j^\dagger a_l a_k - \omega \sum_{ij} j_{ij}^y a_i^\dagger a_j, \tag{1}$$

where $t_{ij} = \langle i|\hat{t}|j\rangle$ gives the matrix elements of single-particle kinetic energies in the basis $|i\rangle$ $(i = 1,2,\dots)$ with corresponding creation and annihilation operators $a_i^\dagger$ and a_j, respectively. $\overline{V}_{ijkl} = \langle ij|\hat{V}|kl\rangle - \langle ij|\hat{V}|lk\rangle$ is the antisymmetrized two-body interaction. In the present work, we choose the Skyrme force for the two-body interaction $\hat{V}(\mathbf{r}_1,\mathbf{r}_2)$. The last term is from the Coriolis force with a rotational frequency ω. We assume that the rotation is around the principle axis y. In the matrix element $j_{ij}^y = \langle i|\hat{j}^y|j\rangle$, $\hat{j}^y$ is the single-particle angular momentum operator projected onto the y axis. All the notation is standard.

Starting with a harmonic oscillator (HO) basis $\{a_i^\dagger, a_i\}$, we can define a HF basis in the body-fixed reference frame by a unitary transformation,

$$b_\mu^\dagger = \sum_i c_{i\mu} a_i^\dagger, \tag{2}$$

where $b_\mu^\dagger(b_\mu)$ is the single-particle creation (annihilation) operator in the body-fixed HF basis, giving single-particle Routhians (i.e., single-particle orbits in the rotating reference frame). The HF wave function in the body-fixed reference frame is written as

$$|G^\omega\rangle = \prod_{\mu=1}^{A} b_\mu^\dagger|-\rangle, \tag{3}$$

where $|-\rangle$ is the vacuum. The wave function $|G^\omega\rangle$ gives the lowest-energy state at a given rotational frequency ω, with a defined symmetry (e.g., with given parity and signature). It should be noted that the HF wave function ignores the residual two-body correlation which is usually treated using the Bogoliubov pairing method. The total HF energy in the cranked reference frame (usually called total Routhian) is obtained by

$$E_G^{\mathrm{HF}}(\omega) = \langle G^\omega|\hat{H}|G^\omega\rangle = \sum_{ij} t_{ij}\rho_{ji}^\omega + \frac{1}{2}\sum_{ijkl}\overline{V}_{ijkl}\rho_{ik}^\omega\rho_{jl}^\omega - \omega\sum_{ij} j_{ij}^y \rho_{ji}^\omega, \tag{4}$$

where $\rho_{ij}^\omega = \langle G^\omega|a_j^\dagger a_i|G^\omega\rangle = \sum_{\mu=1}^{A} c_{i\mu}c_{j\mu}^*$ is the cranked density matrix element written in the deformed HO basis $\{a_i^\dagger, a_i\}$. The HF single-particle eigen wave functions described by $\{c_{i\mu}\}$ are determined by diagonalizing the cranked single-particle HF Hamiltonian,

$$h_{ij}^\omega = t_{ij} - \omega j_{ij}^y + \sum_{kl}\overline{V}_{kilj}\rho_{lk}^\omega. \tag{5}$$

In the wave function $|G^\omega\rangle$ and corresponding energy $E_G^{\mathrm{HF}}(\omega)$, it has been assumed in fact that nucleons occupy the single-particle Routhians from the lowest one to the cranking Fermi surface. Combining Eqs. (4) and (5), we can calculate the yrast rotational band. We repeat that the HF calculation neglects higher-order nucleon correlations, e.g., the residual two-body pairing which is treated usually using the Bogoliubov pairing method. In the present work, we will adopt the PNC pairing method to treat the residual two-body interaction.

Choosing the HF wave function $|G^\omega\rangle$ as a reference state and using Wick's theorem, we can rewrite the cranked total

Hamiltonian (1) as

$$\hat{H}^{\omega} = E_G^{\rm HF}(\omega) + \sum_{ij} h_{ij}^{\omega} : a_i^{\dagger} a_j : + \frac{1}{4} \sum_{ijkl} \overline{V}_{ijkl} : a_i^{\dagger} a_j^{\dagger} a_l a_k : , \tag{6}$$

where $: a_i^{\dagger} a_j :$ and $: a_i^{\dagger} a_j^{\dagger} a_l a_k :$ are the normally ordered products of the creation and annihilation operators. It is required that all annihilation and creation operators which make $|G^{\omega}\rangle$ be zero when acting on $|G^{\omega}\rangle$ are to the right of all other operators which do not make $|G^{\omega}\rangle$ be zero.

If one uses the cranked HF basis in which h_{ij}^{ω} has been already diagonalized, the cranked total Hamiltonian (6) can be expressed in a simple form,

$$\hat{H}^{\omega} = E_G^{\rm HF}(\omega) + \sum_{\mu \geqslant A+1} e_{\mu}^{\omega} b_{\mu}^{\dagger} b_{\mu} - \sum_{\mu=1}^{A} e_{\mu}^{\omega} b_{\mu} b_{\mu}^{\dagger} + \hat{H}', \tag{7}$$

with

$$\hat{H}' = \frac{1}{4} \sum_{\mu_1 \mu_2 \mu_3 \mu_4} \overline{V}_{\mu_1 \mu_2 \mu_3 \mu_4} : b_{\mu_1}^{\dagger} b_{\mu_2}^{\dagger} b_{\mu_4} b_{\mu_3} : , \tag{8}$$

where e_i^{ω} is the single-particle Routhian (i.e., the HF single-particle eigenenergy in the rotating reference frame). In Eq. (7), the second and third terms give particle-hole excitations, with the second term for particle channel and the third one for hole channel. The fourth term $\hat{H}'$ is the residual two-body interaction. For the HF wave function $|G^{\omega}\rangle$ which gives the lowest energy in the body-fixed reference frame, we have $\langle G^{\omega}|\hat{H}'|G^{\omega}\rangle = 0$, which indicates that the residual two-body correlation is not included in $|G^{\omega}\rangle$.

It seems that, by including particle-hole excitations, Hamiltonian (7) can construct various excited configurations with respect to the lowest HF state $|G^{\omega}\rangle$. In the HF theory, an excited configuration in principle can be solved self-consistently by defining its own HF wave function with the specific single-particle orbits occupied or unoccupied. The change of the orbital occupations can result in variation of the HF mean field, which in turn affects the HF single-particle states. Indeed, the self-consistent interplay between the HF mean field and the specific configuration is missing if one ignores the residual two-body correlation $\hat{H}'$ in Eq. (7). In fact, $\hat{H}'$ produces various two-body couplings and leads to various configuration mixings. This is similar to the standard shell model. If the $\hat{H}'$ term is treated exactly, i.e., one calculates the $\hat{H}'$ matrix elements and diagonalizes the full Hamiltonian, the calculation should include the interplay between the HF mean field and the specific configuration. Such an argument has been discussed by Greiner *et al.* [25].

The exact shell-model treatment of $\hat{H}'$ is a tedious work for deformed nuclei. In mean-field model, the residual two-body interaction is usually approximated by the residual pairing interaction. In the present work, we use the PNC method to treat the pairing [16,20].

In a nonrotating basis, the residual pairing interaction is written as

$$H_p = -G \sum_{\xi\eta} a_{\xi}^{\dagger} a_{\bar{\xi}}^{\dagger} a_{\bar{\eta}} a_{\eta}, \tag{9}$$

where $\bar{\xi}(\bar{\eta})$ indicate the time-reversed state. In the rotational case, the time-reversal symmetry is broken, but we can define new good quantum number(s). In the cranking HF solver (named HFODD [26]), three one-dimension HO bases are taken for the three directions of the x, y, and z axes, corresponding to a three-dimension deformed HO basis. In HFODD, the good number is called the simplex, which is defined by $\hat{S}_y = \hat{P} e^{-i\pi \hat{j}_y}$ with $\hat{P}$ being the parity. In quadrupole, hexadecapole, and other even-multipole deformations, both parities and signature ($e^{-i\pi \hat{j}_y}$) are conserved. One can make a transformation from the time-reversal symmetric basis to the simplex basis by [26]

$$\begin{aligned} \beta_{\xi,s=+i}^{\dagger} &= \frac{1}{\sqrt{2}} (i^{n_y} a_{\xi}^{\dagger} - i^{-n_y+1} a_{\bar{\xi}}^{\dagger}), \\ \beta_{\xi,s=-i}^{\dagger} &= \frac{1}{\sqrt{2}} (-i^{n_y+1} a_{\xi}^{\dagger} + i^{-n_y} a_{\bar{\xi}}^{\dagger}), \end{aligned} \tag{10}$$

where n_y is the oscillation quantum number in the y axis. In the simplex basis, the pairing interaction can be written as

$$H_p = -G \sum_{\xi\eta} \beta_{\xi+}^{\dagger} \beta_{\bar{\xi}-}^{\dagger} \beta_{\eta-} \beta_{\bar{\eta}+}, \tag{11}$$

where $\xi+(\xi-)$ represents the basis eigenstate ξ with a positive (negative) simplex, and G is the pairing strength.

In order to reduce the model space, the cranking PNC pairing calculation takes the cranked deformed HF single-particle eigenstates as the model basis for the diagonalization of the full Hamiltonian H^{ω}. The cranked deformed basis can efficiently include cranking- and deformation-sensitive states (e.g., intruder states) and leads to an efficient reduction of the model space which is truncated according to the energies of the cranked many-particle configurations of the model [16]. In the simplex basis, the eigenstates $|\mu s\rangle$ ($\mu = 1,2,\ldots; s = \pm i$) of the cranked deformed HF single-particle Hamiltonian (5) can be expressed as [16]

$$|\mu s\rangle = \sum_{\xi} c_{\mu\xi}(s) |\xi s\rangle, \tag{12}$$

where $|\xi s\rangle$ stands for noncranked deformed HO single-particle eigenstates in the simplex scheme, defined by Eq. (10) (i.e., $\beta_{\xi,s=\pm i}^{+}$). The coefficients $c_{\mu\xi}(s)$ are determined by diagonalizing the Hamiltonian (5) in the simplex basis. In fact, the coefficients are automatically given in the cranking HF calculations [26]. A cranked many-particle configuration of the N-body system can be written as

$$|\mu_1 \mu_2 \cdots \mu_n\rangle = b_{\mu_1}^{\dagger} b_{\mu_2}^{\dagger} \cdots b_{\mu_n}^{\dagger} |-\rangle, \tag{13}$$

where $b_{\mu}^{\dagger}$ is the cranked deformed HF single-particle creation operator that appeared in Eq. (2). According to Eq. (12), we have

$$b_{\mu\pm}^{\dagger} = \sum_{\xi} c_{\mu\xi}(\pm) \beta_{\xi\pm}^{\dagger}, \tag{14}$$

where the sign " $\pm$ " indicates the positive or negative simplex (i.e., $s = +i$ or $-i$). In the cranked simplex basis, therefore, with Eqs. (11) and (14), we derive the residual two-body

pairing interaction as

$$H_p = -G \sum_{\mu\mu'\nu\nu'} f^*_{\mu\mu'} f_{\nu\nu'} b^\dagger_{\mu+} b^\dagger_{\mu'-} b_{\nu-} b_{\nu'+}, \tag{15}$$

with

$$f_{\mu\mu'} = \sum_{\xi\xi'} c^*_{\mu\xi}(+) c_{\mu'\xi'}(-). \tag{16}$$

As mentioned above, the coefficients $c^\dagger_{\mu\xi}(+)$ and $c^\dagger_{\mu\xi}(-)$ have been determined in the cranked HF calculation, which gives single-particle Routhians [26]. The full Hamiltonian (7) is then approximated by

$$\hat{H}^\omega = E_G^{\rm HF}(\omega) + \sum_{\mu \geqslant A+1} e^\omega_\mu b^\dagger_\mu b_\mu - \sum_{\mu=1}^{A} e^\omega_\mu b_\mu b^\dagger_\mu + H_p, \tag{17}$$

with the approximation of $H_p = \hat{H}'$. As explained in Eq. (4), $E_G^{\rm HF}(\omega)$ is the lowest HF total Routhian with a given simplex that is conserved. The eigenstates of the total Hamiltonian $\hat{H}^\omega$ are written as [16]

$$|\psi\rangle^\omega = \sum_i C^\omega_i |i\rangle^\omega, \tag{18}$$

with $\{|i\rangle^\omega;\ i = 1,2,\dots\} = \{|\mu_1\mu_2\cdots\mu_n\rangle;\ \text{scanning}\}$, taking all possible configurations in the truncated space [16]. If there is some symmetry (e.g., conserved simplex or parity and signature, depending on deformation), all the configurations taken in diagonalization should keep the symmetry.

The Hamiltonian (17) is diagonalized in a sufficiently large model space of cranking many-particle configurations. We make a model space truncation by setting a cutoff according to configuration energies; i.e., the model configurations with $E_i - E_0 \leqslant E_c$ are taken into account, with E_i, E_0, and E_c being the energy of the configuration $|i\rangle$, the energy of the lowest configuration, and the cutoff energy, respectively. The coefficient C^ω_i for the eigenstates are obtained in the diagonalization. The total angular momentum J_y of the rotational state $|\psi\rangle^\omega$ is calculated by

$$\langle\psi|\hat{J}_y|\psi\rangle^\omega = \sum_i \left|C^\omega_i\right|^2 \langle i|\hat{J}_y|i\rangle^\omega + 2\sum_{i<j} C^\omega_i C^\omega_j \langle i|\hat{J}_y|j\rangle^\omega, \tag{19}$$

with $\hat{J}_y = \sum \hat{j}_y$.

The practical steps of the numerical calculation are as follows: (i) At each given rotational frequency, we first perform a cranking HF calculation by using the HFODD solver [26], which gives $E_G^{\rm HF}(\omega)$ and the cranked deformed single-particle basis. The HF solver gives a self-consistent deformation at each given frequency by minimizing the cranking HF energy [26]. (ii) Within the cranked deformed HF basis, we perform the PNC calculations; i.e., we construct various cranked many-particle configurations in the truncated model space mentioned above, calculating the $\hat{H}^\omega$ matrix elements and diagonalizing. (iii) By comparing the wave functions of obtained many-particle eigenstates $|\psi\rangle^\omega$, we identify the specific configuration and track it with increasing rotational frequency, which gives the rotational band of the intrinsic configuration. The second and third terms in the full Hamiltonian (17) have been diagonalized already in the cranked basis, while the residual pairing interaction H_p has off-diagonal matrix elements which bring configuration mixings. As discussed above, the cranked deformed HF basis with a truncation of cranking many-particle configurations can leads to a strikingly small model space. We have well tested that a dimension of 800–1000 is sufficient for the calculations of collective rotations [16,27].

In the calculation of a rotational sideband, one of the key steps is to identify and track the specific single-particle Routhians which define the intrinsic configuration at bandhead. With the cranked HF single-particle basis wave functions, we can calculate the expectation (averaged) values of the orbital Nilsson numbers $\Omega[N,n_z,\Lambda]$. The numbers are not conserved, but evolve smoothly with changing rotational frequency or deformation [28]. The calculated Nilsson numbers can be used to track the given single-particle orbits involved in the configuration of the sideband. In practice, there are two alternative methods for the configuration-tracked calculation. At each given frequency, one diagonalizes the full Hamiltonian with the shell-model wave functions defined by Eq. (18). After diagonalizing, the configurations of resulting eigenstates can be identified by looking at the occupation probabilities of orbits using the averaged Nilsson numbers. The investigated state can be found with the specific orbits almost fully occupied (orbital occupation probabilities close to 1) and their partner orbits almost unoccupied (occupation probabilities near zero). There would be several eigenstates corresponding to the given configuration, with similar occupation probabilities of the specific orbits. Always, the lowest one should be taken. The cranked deformed single-particle basis provides a "good" condition to give the "pure" specific configuration, which has been well tested in previous calculations [18–23]. The processes of model diagonalization and configuration identification are repeated at the next rotational frequency, and the given sideband can be established by linking the calculations at different frequencies.

Another alternative method is to adiabatically block the specific orbits in the shell-model wave functions; i.e., keep the given orbits occupied in the wave functions. For example, for a seniority $s = 1$ state in an odd nucleus, one can write the shell-model wave functions as

$$|i\rangle^\omega = b^\dagger_\lambda |\mu_1\mu_2\cdots\mu_{n-1}\rangle \quad (\lambda \neq \mu_1 \neq \mu_2 \neq \cdots \neq \mu_{n-1}), \tag{20}$$

with the λth orbit blocked adiabatically while $|\mu_1\mu_2\cdots\mu_{n-1}\rangle$, scanning all possible shell-model configurations except the blocked orbit [16]. The adiabatic blocking can be achieved by using the averaged Nilsson numbers. For a seniority $s = 2$ state which happens in even nuclei, we have

$$|i\rangle^\omega = b^\dagger_\lambda b^\dagger_\sigma |\mu_1\mu_2\cdots\mu_{n-2}\rangle \quad (\lambda \neq \sigma \neq \mu_1 \neq \mu_2 \neq \cdots \neq \mu_{n-2}). \tag{21}$$

Similarly, we can write the adiabatically blocked wave functions for higher-seniority states. The diagonalizing is processed in a model space with $(n-s)$ unblocked particles, i.e, $\{|\mu_1\mu_2\cdots\mu_{n-s}\rangle\}$, scanning all possible shell-model configurations except the blocked orbits [16]. After diagonalizing, the resulting lowest eigenstate is just the state of the given

configuration. The final results obtained in the two methods should be similar. In the present work, we adopted the first method as described above.

We should mention that the shape polarization effect from the blocked orbits is neglected in the methods described above. As explained already, we take the deformation determined by minimizing the cranking HF energy, which should correspond to the deformation of the yrast state. The polarization effect has been discussed, e.g., in Refs. [29,30]. In soft shapes or high seniorities, the polarization effect can be significant [30]. In the present model, the shape polarization can be included easily by adding the excitation energy from the unpaired orbits in the minimization of the energy against the deformation. The residual pairing should not change the deformation. We will include the shape polarization in our future calculations. The polarization effect would play an important role in the calculations of the electromagnetic quadrupole transitions [29]. However, in the present work, we are investigating low-seniority (two- and four-qp) states in the hard Hf isotopes. Therefore, the polarization effect should be small.

The pairing strength G is determined by the odd-even mass difference using the three-point formula [31]. In the conventional BCS pairing method, the calculated pairing gap is considered to reproduce the experimental odd-even mass difference, which is used to determine the BCS pairing strength. However, it has been pointed out that the pairing gap is not exactly the same as the odd-even mass difference, in which there are blocking and mean-field effects [31,32]. The PNC pairing model does not invoke the quantity of the pairing gap. In the present calculations, both theoretical and experimental odd-even mass differences are calculated using the same formula. Then, the pairing strength G is determined by fitting the experimental odd-even mass difference, which includes the blocking and mean-field effects, as discussed in Refs. [31,32].

III. RESULTS AND DISCUSSIONS

In the present work, we calculate the moments of inertia (MoI) for the yrast bands and the sidebands of broken-pair intrinsic excited states in the Hf isotopes. These nuclei provide a good playground for the theoretical investigations of various rotational bands with rich experimental data available. In the numerical solving of the cranking SHF equations, we took 680 deformed Cartesian HO basis states which cover the HO shells up to $N_x = 13$, $N_y = 13$, and $N_z = 14$. Such a basis space was used in the calculations of transfermium nuclei [33]. Therefore, it should be large enough for the calculation of rare-earth nuclei.

Figure 1 plots the kinematic moments of inertia $\mathcal{J} = J_y/\omega$ for the yrast bands of the hafnium isotopes. For comparison, we have also calculated the MoI's using the cranking Skyrme HFB model with Lipkin-Nogami pairing (indicated by HFB) [37]. In the Skyrme HFB calculations, a volume pairing is used with the strength determined by fitting the odd-even mass difference. In both the HFP and HFB calculations, the Skyrme force of SLY4 [38] is adopted. The cranking HFP calculations reproduce well the experimental MoI's and up-bendings that are caused by the alignment of the $\nu i_{13/2}$ neutrons. The second up-bendings

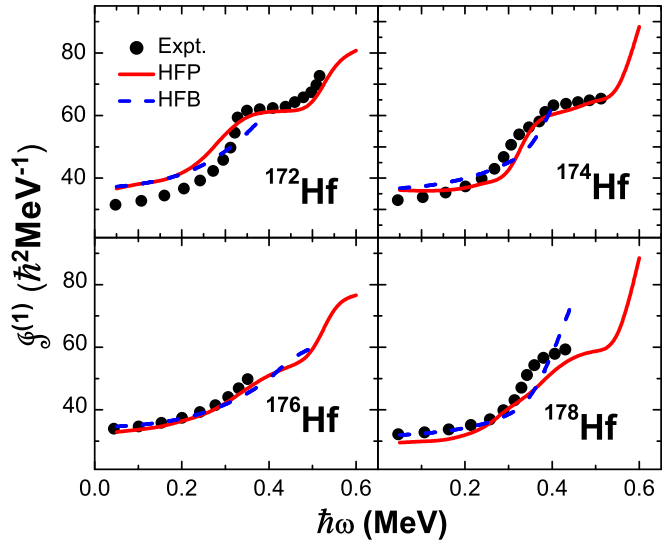

FIG. 1. (Color online) Calculated and experimental MoI's for yrast bands in $^{172-178}$Hf. Experimental MoI's are extracted with data from Refs. [34–36]. The pairing strengths for proton and neutron are $G_p = 0.40$ MeV and $G_n = 0.52$ MeV, respectively, determined by fitting experimental odd-even mass differences. HFP indicates the present Hartree-Fock plus PNC pairing calculations.

around $\hbar\omega \approx 0.55$ MeV are predicted, which are caused by the alignment of the $\pi h_{11/2}$ protons. The second alignment was observed in ^{172}Hf. The cranking HFB calculations stop at $\hbar\omega \approx 0.4$ MeV where the band crossing between the ground-state and first two-quasiparticle (two-qp) bands occurs. For the excited band, the two-qp excitation should be explicitly included in the HFB wave function. By blocking adiabatically the two orbits which cause the alignment, one should be able to obtain the converged HFB solution [39]. The present HFB calculation does not include such a quasiparticle excitation.

In the present HFP calculations for this mass region, we take a cutoff energy of $E_c = 6.2$ MeV which gives a dimension about 800. The pairing strength is determined within the chosen dimension, by fitting the experimental odd-even mass difference. It has been well tested that such a model space is sufficient for the cranking calculations of rotational bands [16,23]. Figure 2 displays the calculated MoI for the ^{172}Hf yrast band at different cutoff energies. Figure 3 gives the plots of energies as a function of angular momentum for the yrast and $K^\pi = 6^+$ and 8^- bands in ^{172}Hf at different cutoffs, compared with experimental data [34,40]. We see that the calculations with $E_c \geqslant 6.2$ MeV (correspondingly dimension $\geqslant$800) give similar results for both MoI's and energies. The calculated bandhead energies of the two excited bands are in good agreement with data. At different cutoffs, the pairing strength G needs to be readjusted to reproduce the experimental odd-even mass difference.

In the mass 180 region, there is an abundance of broken-pair multiquasiparticle states and associated rotational bands (see Refs. [41–45], and references therein). The bands built on excited configurations are called sidebands (relative to the ground-state band), providing rich information for nuclear structure studies. Multiquasiparticle states built on high-Ω

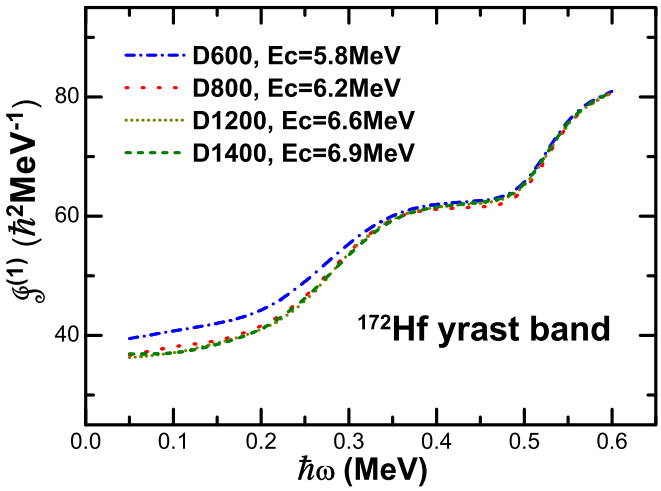

FIG. 2. (Color online) The HFP calculations of MoI for the ^{172}Hf yrast band at different cutoff energies (E_c) which give different model dimensions. D600, D800, D1200, and D1400 indicate the dimensions of 600, 800, 1200, and 1400, respectively.

orbits can form high-K isomers. In the $Z = 72$ Hf isotopes, rotational bands built on the two-proton $\pi 5/2^+[402] \otimes 7/2^+[404]$ ($K^\pi = 6^+$) and $\pi 9/2^-[514] \otimes 7/2^+[404]$ ($K^\pi = 8^-$) configurations have been observed systematically [40,46–49]. Figures 4 and 5 show the calculations of the

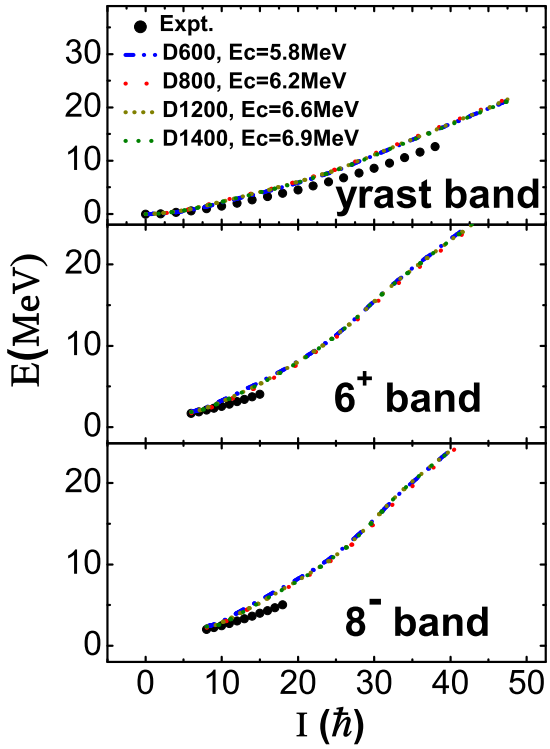

FIG. 3. (Color online) The HFP calculations of energies as a function of angular momentum for the three bands in ^{172}Hf at different cutoffs, compared with experimental data [40]. The configurations are $K^\pi = 6^+ : \pi 5/2^+[402] \otimes \pi 7/2^+[404]$ and $K^\pi = 8^- : \pi 9/2^-[514] \otimes \pi 7/2^+[404]$.

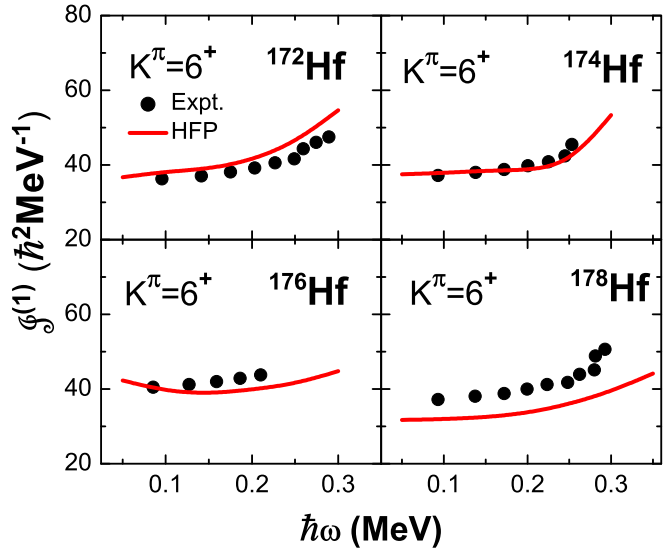

FIG. 4. (Color online) Calculated and experimental MoI's for the $K^\pi = 6^+(\pi 5/2^+[402] \otimes \pi 7/2^+[404])$ bands in $^{172-178}$Hf. Experimental MoI's are obtained with data from Refs. [35,40,46–49].

MoI's for the $K^\pi = 6^+$ and 8^- rotational bands, compared with experimental data. We can see that the present calculations can reproduce the experimental MoI's well. In ^{172,174}Hf, the mixture between the two-proton $K^\pi = 6^+$ ($\pi 5/2^+[402] \otimes \pi 7/2^+[404]$) and two-neutron $K^\pi = 6^+$ ($\nu 7/2^-[514] \otimes 5/2^-[512]$) configurations is weak [46,50], while the mixture becomes obvious with increasing the neutron number [47,49]. This may be the reason to explain the difference between the calculated and experimental MoI's in ^{178}Hf. In the cranking shell model, the band mixture (between different bands) is not included.

Figure 5 displays the MoI's of the $K^\pi = 8^-$ rotational bands which are built on the $\pi 9/2^-[514] \otimes 7/2^+[404]$

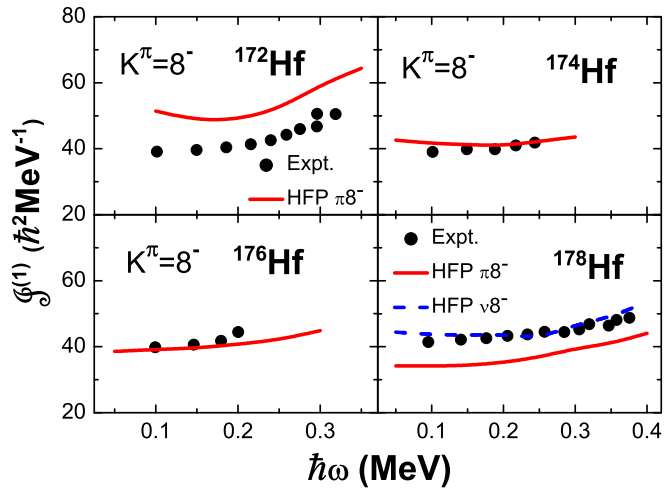

FIG. 5. (Color online) Calculated and experimental MoI's for the two-proton $K^\pi = 8^-(\pi 9/2^-[514] \otimes \pi 7/2^+[404])$ bands in $^{172-178}$Hf. For ^{178}Hf, the two-neutron $K^\pi = 8^-(\nu 7/2^-[514] \otimes 9/2^+[624])$ band is also calculated. Experimental MoI's are obtained with data from Refs. [35,40,46–49].

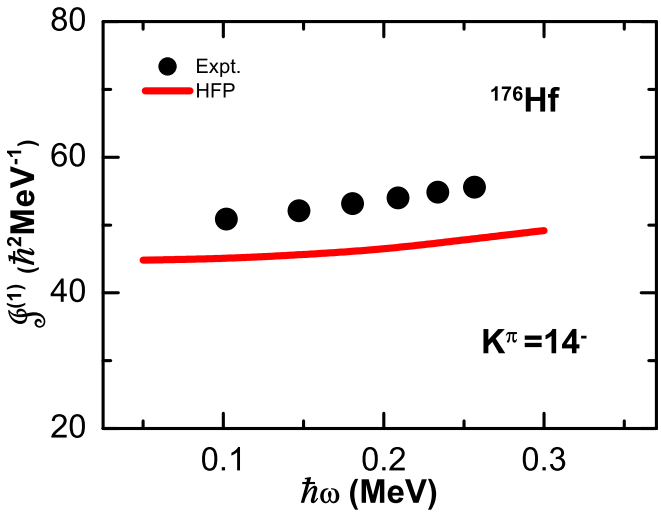

FIG. 6. (Color online) Calculated and experimental MoI's for the $K^\pi = 14^-$ ($\pi\{9/2^-[514],7/2^+[404]\} \otimes \nu\{7/2^-[514] \otimes 5/2^-[512]\}$) bands in ^{176}Hf. Experimental MoI's are obtained with data from Ref. [53].

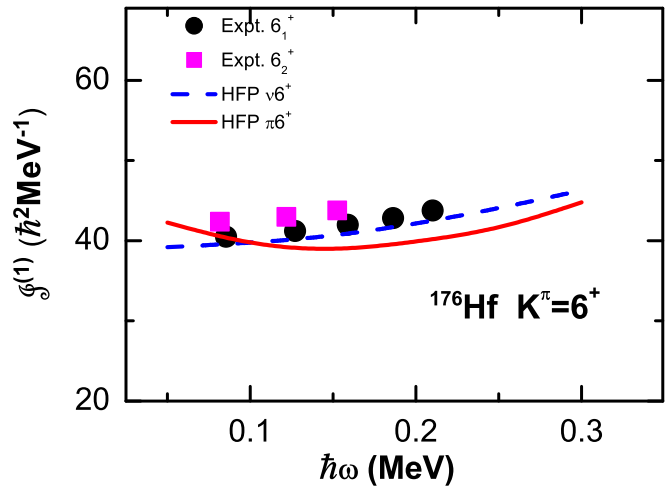

FIG. 7. (Color online) Calculated and experimental MoI's for the two $K^\pi = 6^+$ bands in ^{176}Hf. The proton or neutron $K^\pi = 6^+$ configurations are $\pi 5/2^+[402] \otimes \pi 7/2^+[404]$ or $\nu 7/2^-[514] \otimes 5/2^-[512]$, respectively. Experimental MoI's are obtained with data in Ref. [47].

configuration in $^{172-178}$Hf as a function of rotational frequency. The self-consistent configuration-constrained cranking Skyrme HF calculations with the PNC pairing give reasonable results compared with data. In Refs. [40,46,47,51], it was commented that the $K^\pi = 8^-$ states have a relatively pure two-proton $\pi 9/2^-[514] \otimes 7/2^+[404]$ configuration in ^{172,174,176}Hf with a small admixture of a two-neutron $K^\pi = 8^-$ ($\nu 9/2^+[624] \otimes 7/2^-[514]$) configuration, while the mixture becomes obvious in ^{178}Hf. Different configuration admixtures were suggested for the low 8^- band in ^{178}Hf, according to the different choices of the rotational gyromagnetic factors [49]. To give an insight into the configuration of the observed 8^- band, we have also calculated the neutron 8^- configuration using the present HFP method, shown in Fig. 5. It seems that the two-neutron 8^- configuration gives a better quantitative description of the data. The mixing between $\pi 8^-$ and $\nu 8^-$ is possible. Further, the two-proton $\pi 9/2^-[514] \otimes 7/2^+[404]$ configuration coupling to the two-neutron $\nu 7/2^-[514] \otimes 5/2^-[512]$ makes a four-quasiparticle $K^\pi = 14^-$ state, which was observed to be an isomer at an energy of 2866 keV with a half-life of 401 μs in ^{176}Hf [52], and a built-on rotational band was identified [53]. Figure 6 shows the calculated rotational moment of inertia for the observed $K^\pi = 14^-$ band in ^{176}Hf, giving a reasonable agreement with experimental MoI extracted from data [53].

In the mass 180 region, many phenomena were observed to be related to band mixing, configuration mixing, and K-forbidden electromagnetic decays [40,49,54–56]. It is believed that the K-selection rule governs the decays of high-K bands, such that γ-ray transitions involving large changes in K values are forbidden. The violation of the K selection indicates the K mixing associated with nonaxial deformations or the Coriolis force. For example, two $K^\pi = 6^+$ band were observed in ^{176}Hf [47]. It is special that no intraband transition is observed in the 6_2^+ band with a bandhead energy at 1761 keV [47]. In Fig. 7, we have calculated for both the proton and neutron $K^\pi = 6^+$ configurations, compared with experimental bands. The calculated MoI's of the two 6^+ configurations are close to each other (agreeing with data as well). This would imply a strong mixing of the two configurations in the observed 6_1^+ and 6_2^+ bands, supported by the experimental observation of the strong interband electromagnetic transitions from the members of the 6_2^+ band to those of the 6_1^+ band [47]. From the MoI calculations, we might assign that the 6_1^+ band should mainly possess the proton $\pi 5/2^+[402] \otimes \pi 7/2^+[404]$ configuration and the 6_2^+ band has a major component of the neutron $\nu 7/2^-[514] \otimes 5/2^-[512]$ configuration, with configuration mixing between them.

In the Hf isotopes, one of the most remarkable isomers is the second metastable state ^{178}Hf^{m2} observed in the nucleus ^{178}Hf. The isomer lies at 2.4 MeV above the ground state, and has angular momentum and parity $I^\pi = K^\pi = 16^+$ with a half-life of 31 years [57,58]. The configuration is assigned with one broken neutron pair ($\nu 7/2^-[514] \otimes 9/2^+[624]$) and a proton pair ($\pi 7/2^+[404] \otimes 9/2^-[514]$), both coupling to $I^\pi = 8^-$. The exceptionally long lifetime of this isomer is not only because of its low excitation energy compared with other states around $I = 16$, but also its high-K value which largely forbids electromagnetic decays into lower K states. We have calculated the MoI of the ^{178}Hf $K^\pi = 16^+$ band, shown in Fig. 8, giving a good agreement with data. A constant MoI would imply a pure configuration, which was already commented on in the experimental paper [49].

It should be explained in more details that, in the calculations above, we performed the HF and pairing calculations by two separate processes. We first run the cranking HF iterations, obtaining the converged HF solution. Then, with the obtained HF density, the full Hamiltonian is diagonalized with the pairing interaction. Such a calculation is time saving, but neglects the interplay between the HF mean field and pairing correlation. The interplay would be important, which may result in the change of the order of single-particle levels.

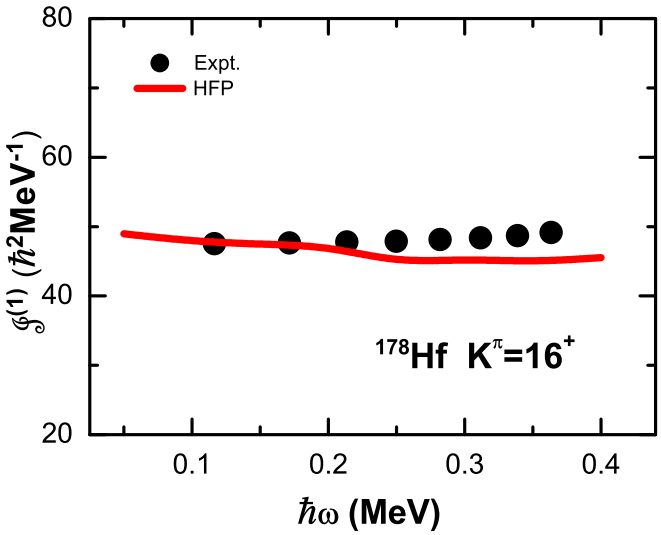

FIG. 8. (Color online) Calculated and experimental MoI's for the famous $K^{\pi} = 16^{+}$ band in ^{178}Hf. Experimental MoI's are extracted with data from Ref. [35].

In the present model, this interplay can be taken into account by processing density iterations. The detailed steps of the iterations are as follows: (i) For each given frequency, we first run an one-step cranking HF iteration (in this stage the HF solution has not been converged). After the one-step HF iteration, we calculate pairing matrix elements using Eqs. (15) and (16). Then the full Hamiltonian with pairing is diagonalized, which gives a new density that includes the pairing effect. (ii) The new density is put back into the HF equations for another HF iteration, giving another new density. Such iterations are repeated until a converged density is obtained. Such a calculation includes the interplay between the HF mean field and pairing correlation. We indeed see that the interplay can cause a change of the order of some single-particle levels.

Figure 9 and 10 display comparisons between the two types of calculations with and without the density iteration.

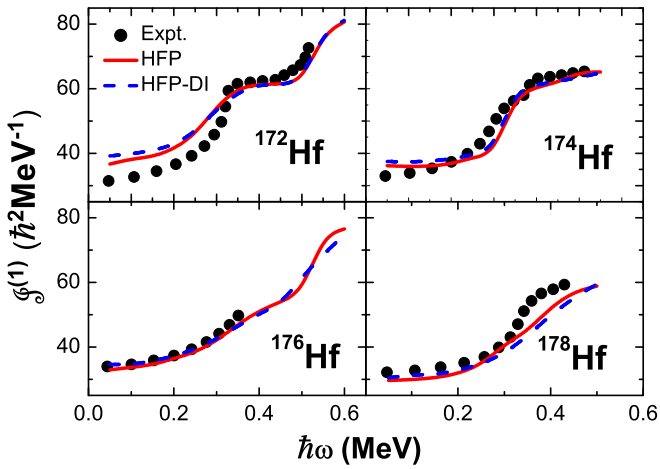

FIG. 9. (Color online) Comparisons of calculations with and without the density iteration (DI), indicated by HFP-DI and HFP, respectively, for the yrast bands in $^{172-178}$Hf.

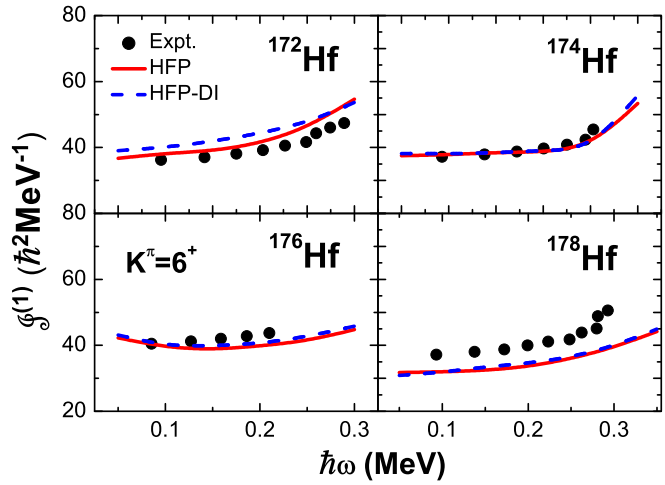

FIG. 10. (Color online) Similar to Fig. 9, but for the $K^{\pi} = 6^{+}(\pi 5/2^{+}[402] \otimes \pi 7/2^{+}[404])$ bands.

Resulting differences seem small for both the yrast and high-K bands. For the investigated Hf isotopes, the differences in binding energy calculations are less than 0.1%. The differences in high-K excitation energy calculations are less than 200 keV. The density iteration calculation is much time-consuming. However, we should perform the self-consistent density iteration calculations in our future works.

IV. SUMMARY

We have developed a configuration-constrained cranking calculation within the Skyrme Hartree-Fock plus particle-number-conserving pairing. The PNC pairing takes the technique of the shell-model diagonalization. The cranked deformed HF basis gives an efficient inclusion of all important configurations (e.g., the deformation- and rotation-sensitive intruder states) in a rather small model space. The given configuration can be identified and tracked by using the wavefunctions of the PNC diagonalization, giving a rotational band built on the specific configuration.

The cranking Skyrme Hartree-Fock pairing calculation has been successfully applied to the investigations of the yrast bands and sidebands of hafnium isotopes, well reproducing the moments of inertia and up-bending properties. The rotational bands built on $K^{\pi} = 6^{+}$ and 8^{-} isomers in $^{172-178}$Hf isotopes have been analyzed. The rotation of the famous ^{178}Hf $K^{\pi} = 16^{+}$ $T_{1/2} = 31$yr isomer has been calculated, with the experimental moment of inertia reproduced well.

ACKNOWLEDGMENTS

This work is supported by the National Key Basic Research Program of China under Grant No. 2013CB834402, the National Natural Science Foundation of China under Grants No. 11235001, No. 11320101004 and No. 11575007, and the Open Project Program of State Key Laboratory of Theoretical Physics, Institute of Theoretical Physics, Chinese Academy of Sciences, China (Grant No. Y4KF041CJ1).

[1] W. Satula, R. Wyss, and P. Magierski, Nucl. Phys. A **578**, 45 (1994).
[2] T. Bengtsson and I. Ragnarsson, Nucl. Phys. A **436**, 14 (1985).
[3] M. Bender, P.-H. Heenen, and P.-G. Reinhard, Rev. Mod. Phys. **75**, 121 (2003).
[4] A. V. Afanasjev, J. König, and P. Ring, Nucl. Phys. A **608**, 107 (1996).
[5] B. R. Mottelson and J. G. Valatin, Phys. Rev. Lett. **5**, 511 (1960).
[6] N. Pillet, P. Quentin, and J. Libert, Nucl. Phys. A **697**, 141 (2002).
[7] B. Banerjee, H. J. Mang, and P. Ring, Nucl. Phys. A **215**, 366 (1973).
[8] F. Grümmer, K. W. Schmid, and A. Faessler, Nucl. Phys. A **308**, 77 (1978).
[9] U. Mutz and P. Ring, J. Phys. G **10**, L39 (1984).
[10] D. Vretenar, A. V. Afanasjev, G. A. Lalazissis, and P. Ring, Phys. Rep. **409**, 101 (2005).
[11] M. Anguiano, J. L. Egido, and L. M. Robledo, Nucl. Phys. A **696**, 467 (2001).
[12] J. A. Sheikh and P. Ring, Nucl. Phys. A **665**, 71 (2000).
[13] M. Anguiano, J. L. Egido, and L. Robledo, Phys. Lett. B **545**, 62 (2002).
[14] H. Molique and J. Dudek, Phys. Rev. C **56**, 1795 (1997).
[15] R. Wyss and W. Satula, Phys. Lett. B **351**, 393 (1995).
[16] X. M. Fu, F. R. Xu, J. C. Pei, C. F. Jiao, Y. Shi, Z. H. Zhang, and Y. A. Lei, Phys. Rev. C **87**, 044319 (2013).
[17] J. Y. Zeng and T. S. Cheng, Nucl. Phys. A **405**, 1 (1983).
[18] J. Y. Zeng, T. H. Jin, and Z. J. Zhao, Phys. Rev. C **50**, 1388 (1994).
[19] J. Y. Zeng, S. X. Liu, L. X. Gong, and H. B. Zhu, Phys. Rev. C **65**, 044307 (2002).
[20] X. Wu, Z. H. Zhang, J. Y. Zeng, and Y. A. Lei, Phys. Rev. C **83**, 034323 (2011).
[21] Z. H. Zhang, Y. A. Lei, and J. Y. Zeng, Phys. Rev. C **80**, 034313 (2009).
[22] Z.-H. Zhang, J.-Y. Zeng, E.-G. Zhao, and S.-G. Zhou, Phys. Rev. C **83**, 011304(R) (2011).
[23] X. M. Fu, F. R. Xu, C. F. Jiao, W. Y. Liang, J. C. Pei, and H. L. Liu, Phys. Rev. C **89**, 054301 (2014).
[24] W. Nazarewicz, R. Wyss, and A. Johnson, Nucl. Phys. A **503**, 285 (1989).
[25] W. Greiner and J. A. Maruhn, *Nuclear Models* (Springer, Berlin, 1996).
[26] J. Dobaczewski and J. Dudek, Comput. Phys. Commun. **102**, 166 (1997).
[27] S. X. Liu, T. Li, and B. R. Chen, Phys. Rev. C **80**, 044329 (2009).
[28] F. R. Xu, P. M. Walker, J. A. Sheikh, and R. Wyss, Phys. Lett. B **435**, 257 (1998).
[29] L. B. Karlsson, I. Ragnarsson, and S. Åberg, Nucl. Phys. A **639**, 654 (1998).
[30] F. R. Xu, P. M. Walker, and R. Wyss, Phys. Rev. C **59**, 731 (1999).
[31] W. Satuła, J. Dobaczewski, and W. Nazarewicz, Phys. Rev. Lett. **81**, 3599 (1998).
[32] F. R. Xu, R. Wyss, and P. M. Walker, Phys. Rev. C **60**, 051301(R) (1999).
[33] Y. Shi, J. Dobaczewski, and P. T. Greenlees, Phys. Rev. C **89**, 034309 (2014).
[34] http://www.nndc.bol.gov/.
[35] A. B. Hayes, D. Cline, C. Y. Wu, A. M. Hurst, M. P. Carpenter, J. P. Greene, R. V. F. Janssens, T. Lauritsen, D. Seweryniak, S. Zhu, S. A. Karamian, P. M. Walker, T. P. D. Swan, S. V. Rigby, D. M. Cullen, N. M. Lumley, P. Mason, J. J. Carroll, B. Detwiler, T. Harle, I. Mills, and G. Trees, Int. J. Mod. Phys. E **20**, 474 (2011).
[36] R. B. Firestone and V. S. Shirley, *Table of Isotopes* (Wiley, New York, 1996).
[37] J. Dobaczewski and P. Olbratowski, Comput. Phys. Commun. **158**, 158 (2004).
[38] E. Chabanat, P. Bonche, P. Haensel, J. Meyer, and R. Schaeffer, Nucl. Phys. A **635**, 231 (1998).
[39] B. G. Carlsson, I. Ragnarsson, R. Bengtsson, E. O. Lieder, R. M. Lieder, and A. A. Pasternak, Phys. Rev. C **78**, 034316 (2008).
[40] D. M. Cullen, C. Baktash, M. J. Fitch, I. Frosch, R. W. Gray, N. R. Johnson, I. Y. Lee, A. O. Macchiavelli, W. Reviol, X.-H. Wang, and C.-H. Yu, Phys. Rev. C **52**, 2415 (1995).
[41] P. M. Walker, G. D. Dracoulis, A. P. Byrne, B. Fabricius, T. Kibedi, A. E. Stuchbery, and N. Rowley, Nucl. Phys. A **568**, 397 (1994).
[42] P. M. Walker, G. D. Dracoulis, A. P. Byrne, B. Fabricius, T. Kibédi, and A. E. Stuchbery, Phys. Rev. Lett. **67**, 433 (1991).
[43] G. D. Dracoulis, F. G. Kondev, G. J. Lane, A. P. Byrne, T. R. McGoram, T. Kibédi, I. Ahmad, M. P. Carpenter, R. V. F. Janssens, T. Lauritsen, C. J. Lister, D. Seweryniak, P. Chowdhury, and S. K. Tandel, Phys. Rev. Lett. **97**, 122501 (2006).
[44] P. M. Walker, Phys. Scr., T **5**, 29 (1983).
[45] P. M. Walker, G. D. Dracoulis, A. Johnston, and J. R. Leigh, Nucl. Phys. A **293**, 481 (1977).
[46] N. L. Gjørup, P. M. Walker, G. Sletten, M. A. Bentley, B. Fabricius, and J. F. Sharpey-Schafer, Nucl. Phys. A **582**, 369 (1995).
[47] T. L. Khoo, J. C. Waddington, R. A. O'Neil, Z. Preibisz, D. G. Burke, and M. W. Johns, Phys. Rev. Lett. **28**, 1717 (1972).
[48] E. Achterberg, O. A. Capurro, and G. V. Marti, Nucl. Data Sheets **110**, 1473 (2009).
[49] A. B. Hayes, D. Cline, C. Y. Wu, H. Ai, H. Amro, C. Beausang, R. F. Casten, J. Gerl, A. A. Hecht, A. Heinz, H. Hua, R. Hughes, R. V. F. Janssens, C. J. Lister, A. O. Macchiavelli, D. A. Meyer, E. F. Moore, P. Napiorkowski, R. C. Pardo, C. Schlegel, D. Seweryniak, M. W. Simon, J. Srebrny, R. Teng, K. Vetter, and H. J. Wollersheim, Phys. Rev. C **75**, 034308 (2007).
[50] D. M. Cullen, A. T. Reed, D. E. Appelbe, A. N. Wilson, E. S. Paul, R. M. Clark, P. Fallon, I. Y. Lee, A. O. Macchiavelli, and R. W. MacLeod, Nucl. Phys. A **638**, 662 (1998).
[51] M. B. Smith, P. M. Walker, G. C. Ball, J. J. Carroll, P. E. Garrett, G. Hackman, R. Propri, F. Sarazin, and H. C. Scraggs, Phys. Rev. C **68**, 031302(R) (2003).
[52] T. L. Khoo, F. M. Bernthal, R. A. Warner, G. F. Bertsch, and G. Hamilton, Phys. Rev. Lett. **35**, 1256 (1975).
[53] T. L. Khoo, F. M. Bernthal, R. G. H. Robertson, and R. A. Warner, Phys. Rev. Lett. **37**, 823 (1976).
[54] P. M. Walker, G. D. Dracoulis, A. P. Byrne, T. Kibèdi, and A. E. Stuchbery, Phys. Rev. C **49**, 1718 (1994).
[55] G. Mukherjee, P. Chowdhury, F. G. Kondev, P. M. Walker, G. D. Dracoulis, R. D'Alarcao, I. Shestakova, K. Abu Saleem, I. Ahmad, M. P. Carpenter, A. Heinz, R. V. F. Janssens, T. L. Khoo, T. Lauritsen, C. J. Lister, D. Seweryniak, I. Wiedenhoever, D. M. Cullen, C. Wheldon, D. L. Balabanski, M. Danchev,

T. M. Goon, D. J. Hartley, L. L. Riedinger, O. Zeidan, M. A. Riley, R. A. Kaye, and G. Sletten, Phys. Rev. C **82**, 054316 (2010).

[56] A. B. Hayes, D. Cline, C. Y. Wu, J. Ai, H. Amro, C. Beausang, R. F. Casten, J. Gerl, A. A. Hecht, A. Heinz, R. Hughes, R. V. F. Janssens, C. J. Lister, A. O. Macchiavelli, D. A. Meyer, E. F. Moore, P. Napiorkowski, R. C. Pardo, C. Schlegel, D. Seweryniak, M. W. Simon, J. Srebrny, R. Teng, K. Vetter, and H. J. Wollersheim, Phys. Rev. Lett. **96**, 042505 (2006).

[57] P. M. Walker and G. D. Dracoulis, Nature (London) **399**, 35 (1999).

[58] R. G. Helmer and C. W. Reich, Nucl. Phys. A **211**, 1 (1973).